V European Conference on Computational Fluid Dynamics
ECCOMAS CFD 2010
J. C. F. Pereira and A. Sequeira (Eds)
Lisbon, Portugal, 14–17 June 2010

TRANSIENT FLOW ANALYSIS BY IMAGING METHODS – VORONOÏ PARTICLE TRACKING VELOCIMETRY APPLIED TO THE DAM BREAK FLOW

R. Aleixo[*], S. Soares-Frazão[†], and Y. Zech[††]
[*] Institute of Mechanics, Materials and Civil Engineering, Department of Civil and Environmental Engineering, Université catholique de Louvain
Place du Levant 1, 1348 Louvain-la-Neuve, Belgium
e-mail: rui.aleixo@student.uclouvain.be

[†] Fonds National de Recherche and [††]Institute of Mechanics, Materials and Civil Engineering
Department of Civil and Environmental Engineering, Université catholique de Louvain
Place du Levant 1, 1348 Louvain-la-Neuve, Belgium
e-mail: s.soares-frazao@uclouvain.be
e-mail: yves.zech@uclouvain.be

Key words: Dam break, Particle Tracking Velocimetry, Voronoï Tesselation

Abstract. *The introduction of measurement techniques based on imaging techniques,, such as Particle Image Velocimetry, allow to shed a new light on the experimental approach to Fluid Mechanics. They revealed to be quite suited to the study of transitory flows since those techniques can combine both spatial and temporal resolution. In this paper an application of imaging techniques is made to a dam break flow, which is an extreme example of a transient flow. To obtain quantitative information from flow images a Particle Tracking Velocimetry algorithm was used. This algorithm based on the Voronoï Tesselation was shown to be capable of dealing with the strong velocity and free-surface elevation gradients present in such flows. Moreover it takes advantage of the fact that the Voronoï construction is adaptive to density gradients, thus being able to cope with non-uniform seeding particles distributions in the flow. Since by nature the raw PTV data are randomly distributed, a binning technique is applied as post-processing to obtain structured measured data, best suited for further analysis. This binning process consists in splitting the flow field in regular boxes and for each box calculating the average velocity. Its advantages and disadvantages when compared to other data structuring methods, e.g., interpolation towards a pre-defined grid are discussed. In addition, in order to assess the performances of the PTV algorithm, a set of raw flow images were processed with commercial Particle Image Velocimetry software. Finally the results obtained for the flow field are analyzed and the time evolution of the velocity profiles at precise locations of the flow is depicted.*

1 INTRODUCTION

A dam break flow is an example of a severe transient flow where different temporal and spatial scales are present. The applications of such kind of flow are usually related with dam and dyke failure risk assessment. For the experimental study of such flows robust measurement techniques are required due to the different and highly variable temporal and spatial scales existing in the flow. On other hand, the transitory character constrains the use of intrusive techniques such as point-wise devices to obtain the velocity. Full field techniques, like imaging based techniques must thus be used.

For extracting velocity information out of flow-field images two strategies are commonly used. One is the Particle Image Velocimetry (PIV) approach where image correlation is used to determine the flow field [1]. The other is the Particle Tracking Velocimetry (PTV) approach where individual particles are tracked between successive frames [2]. Both approaches have their advantages and disadvantages. PIV is suitable for high particles concentration while PTV performs better for low particles concentrations. Since PIV is founded on image correlation it is usually faster than the PTV. However, since PTV tracks single particles, it is capable of higher spatial resolutions.

In this paper a Voronoï based Particle Tracking Algorithm [3, 4] is presented and its application to a dam break flow is discussed and compared with the results obtained trough a PIV code. Due to the random distribution of the particles in the flow, results issued from a PTV analysis are referred to a non structured grid. In order to compare these results with other experiments it is necessary to refer the data to a structured grid. To do so a binning process is used. This process consists in dividing the obtained non-structured flow field in regular bins, and for each calculates an average of the flow field within. This binning method is compared with the interpolation to a predefined regular grid and the results are discussed.

Finally velocity profiles obtained for the dam-break flow are processed and presented for different time steps.

2 DAM BREAK FLOW

After a sudden rupture of one of the walls of a large water reservoir (such as a dam or a dyke) a dam-break wave occurs that will propagate. This flow has been studied since the last years of the XIX century by Ritter [5] who derived an analytical solution for an idealised case of infinite water reservoir, and infinite channel length. Ritter's work however only describes the macro-scale variables of the flow: water wave celerity and water height evolution, thus nothing referring to the local velocity field. The shear stress between the moving fluid and the wall isn't analyzed by Ritter since the fluid is assumed to be perfect. The risk assessment studies for a dam demands the knowledge of the propagation of the dam break wave over the river bed for which the idealised Ritter model is clearly not sufficient [6].

Many experimental studies have been conducted on the topic of the dam-break flow [6, 7] but due to experimental limitations these were also focused on the macro-scale variables such as water height evolution and wave celerity. Nowadays with the available technology is possible to go further and measure directly the dam-break flow velocity field. In Figure 1 different stages of a dam break flow are presented, issued from experiments at the Hydraulics Laboratory of the Université catholique de Louvain, Belgium. The transitory character of this type of flow is clearly seen from Figure 1. After the dam breaks (Figure 1b) the free surface undergoes a rapid variation seen by the steep frontiers on Figure 1c. This stage was called the Near Field regime [3]. The water waves propagates and the water surface slope becomes gradually mild (Figure 1d)

until the flow can be considered as quasi-steady (Figure 1e and 1f)), also designated as the Far Field regime.

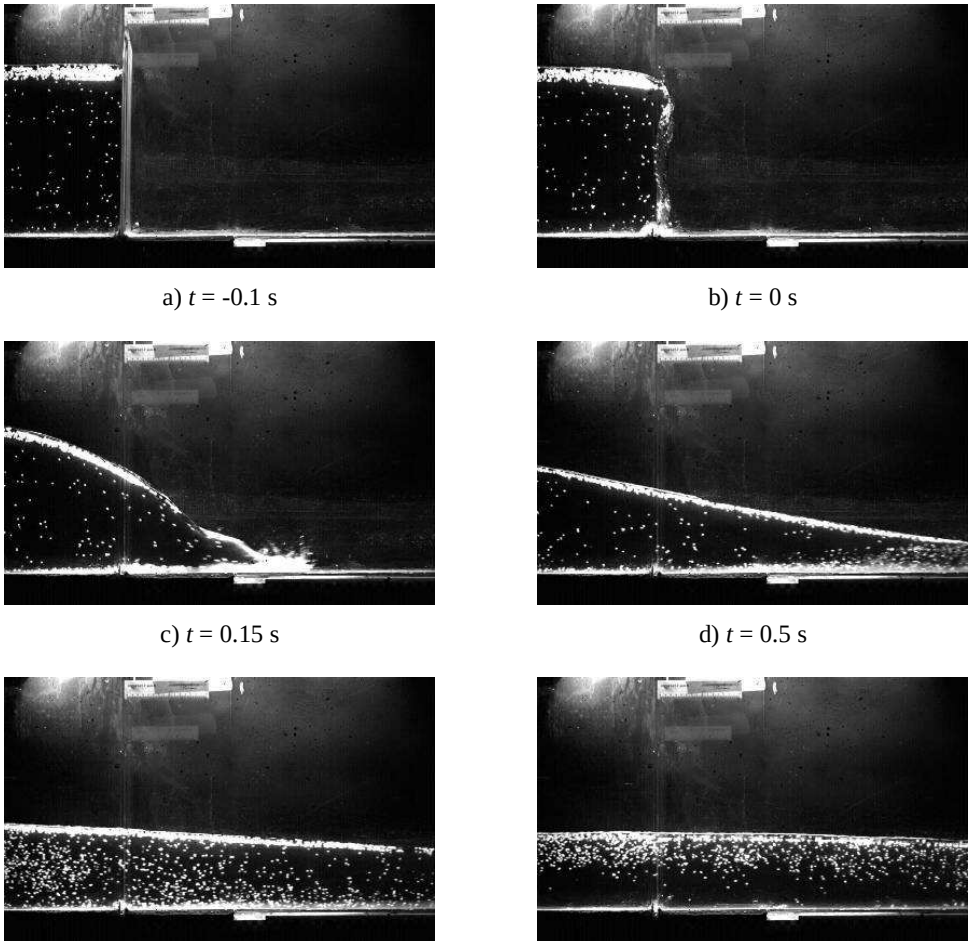

a) t = -0.1 s b) t = 0 s

c) t = 0.15 s d) t = 0.5 s

e) t = 3.5 s f) t = 7 s

Figure 1: Different instants of a dam break flow with an initial water height of 0.325 m. Seeded particles added to allow velocity measurements, as described below.

The scaling variables in the dam break flow are the initial water height, h_0 and gravity acceleration, g, as stated by Stoker [5]. With these variables the following scales can be defined:

$$T_0 = \sqrt{\frac{h_0}{g}} \tag{1}$$

$$c_0 = \sqrt{g h_0} \tag{2}$$

where T_0 is the time scale and c_0 is the velocity scale for a dam break flow. With these scales the non-dimensional variables of a dam break flow are:

$$X = \frac{x}{h_0} \ , \quad Z = \frac{z}{h_0} \tag{3, 4}$$

$$U = \frac{u}{c_0} \ , \quad W = \frac{w}{c_0} \tag{5, 6}$$

$$T = \frac{t}{T_0} \tag{7}$$

where x is the abscissa, z the vertical coordinate, u the longitudinal velocity, w the vertical velocity component and t is the time.

3 VORONOÏ PARTICLE TRACKING VELOCIMETRY

In Figure 1a to 1f it is possible to see the seeded particles in the water, that will be used to determine the velocity field by means of a tracking particle algorithm presented by Capart et al. [4] and adapted to hydrodynamic dam-break flows by Aleixo et al. [3]. This algorithm can be divided in three steps: a) particle detection, b) Voronoï particle tracking and c) tracked particles validation and filtering.

3.1 Particle Detection

The detection scheme is an important part of a particle tracking algorithm since it has to be capable of detect the particles centres to about a fraction of pixel in order to provide accurate velocity results. The particles are assumed to be spherical. The provided lightning is such that it allows the particles to contrast with the surrounding fluid (Figure 1). Images are recorded in a grey level map. The detection scheme consists in the application of different types of filters [4] to determine the particles centres. For exemplification of the particle detection procedure let one consider the raw image of the dam break flow corresponding to $T = 1$ and represented in Figure 2. The first filter to be applied is a low pass filter under the form of a Mexican hat filter to smoothen the image, reducing in such a way the impact of irregularities and parasitic reflections. The result is depicted in Figure 3. Finally a Laplace operator is applied in order to highlight the particles centroids [4]. The particles centres are determined with a subpixel resolution by fitting a parabola along the x and y directions grey levels.

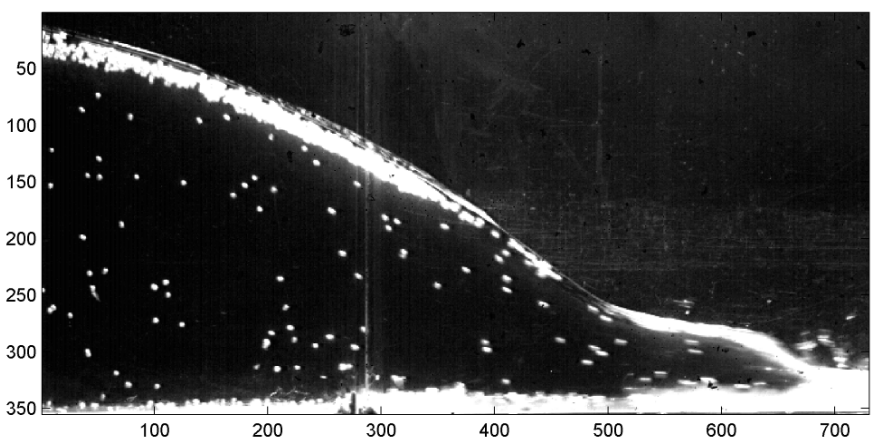

Figure 2: Raw image of a dam break flow for $T = 1$. Axis co-ordinates in pixels.

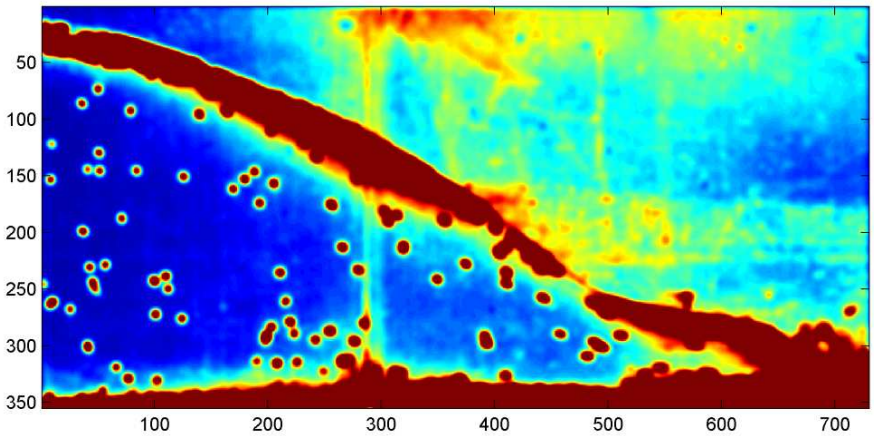

Figure 3: Application of the smoothing operator for $T = 1$. Axis co-ordinates in pixels.

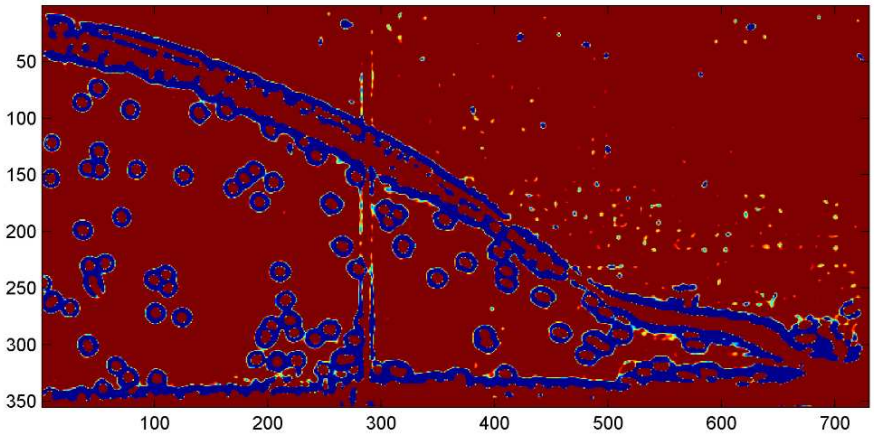

Figure 4: Application of the Laplace operator for $T = 1$. Axis co-ordinates in pixels.

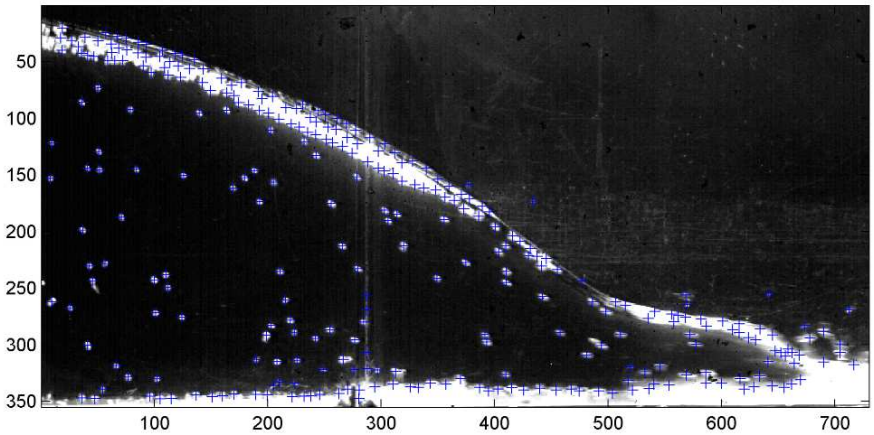

Figure 5: Detected particles position for $T = 1$. Axis co-ordinates in pixels.

3.2 Voronoï Tracking Scheme

After the identification of the particles position in the flow images, each individual particle will be tracked from one image to the other. There are several ways of tracking particles between each frame. One of them is the least displacement method [8] where the matching is made by searching the nearest particle of the foreseen position. Let F1 and F2 be two consecutive frames of the flow. Let $P_{n,1}$ be the *n*-th particle in frame F1 and $P_{m,2}$ the *m*-th particle in frame F2 whose position vectors are given respectively by $\mathbf{r}_{n,1}$ and $\mathbf{r}_{m,2}$. Assuming a small time interval between consecutive images it is reasonable to assume that the particles displacement is small this fact is the basis of the least displacement algorithm. This algorithm searches the nearest particle within a given search area, *S*, of the foreseen particle location as illustrated in Figure 6.

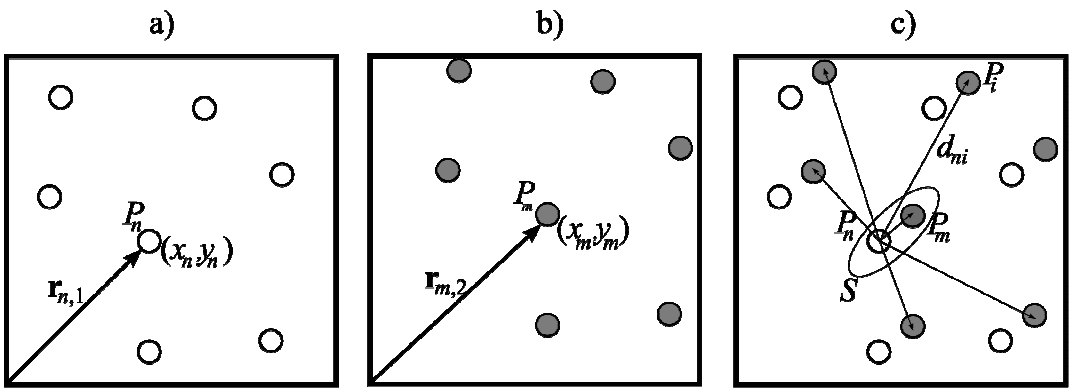

Figure 6: Velocity field and bin division of the flow image.

This method has however some disadvantages. It is not suitable when dealing with high concentration flows since there will be too many particles inside the search area to make a unique choice. Another limitation arises when dealing with intense flow gradients since these can lead to important particles displacements in a short length scale. To overcome these problems Capart et al. [4] proposed a tracking approach based on the Voronoï tessellation of the flow images. In this approach a Voronoï polygon is constructed around each detected particle (Figures 7a and 7b). The union of the different centres will form a so called Voronoï star, and instead of tracking individual particles, the Voronoï PTV algorithm will instead track the Voronoï stars. These steps are represented in Figure 7.

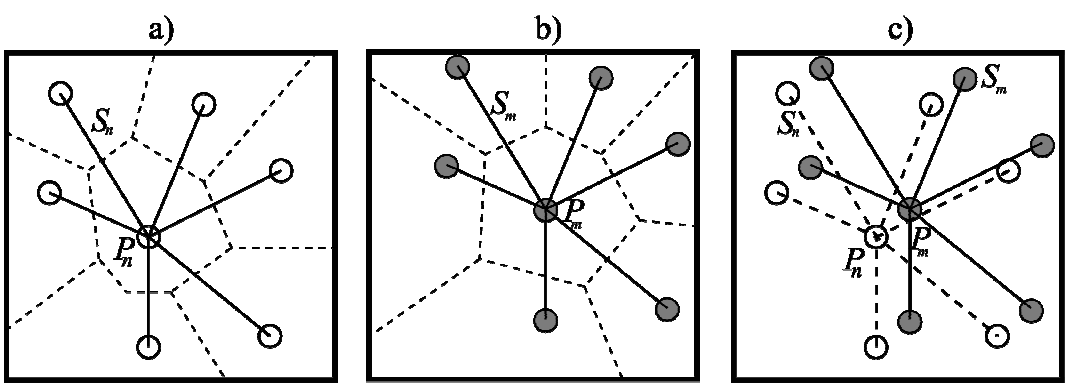

Figure 7: a) and b) Voronoï diagram and Voronoï star representation for two consecutive frames; c) overlap of the two consecutive frames and illustration of the Voronoï star displacement

Therefore the Voronoï star associated with each of the featured points $P_{m,2}$ is compared with the one associated with the one of $P_{n,1}$. An expression for the best match of point $P_{n,1}$ is given in [4] as:

$$\text{match}(P_{n,1}) = \min_{P_{m,2} \in S_{j,2}} \left(\text{dist}_S(S_{n,1}, S_{m,2})\right) \tag{8}$$

where $\text{dist}_S(S_{n.1}, S_{m,2})$ is the *star-distance* that measures the degree of discrepancy between the patterns formed by the two stars, $S_{n,1}$ and $S_{m,2}$. As depicted in Figure 8 this star distance is defined as the median of the distances between the star extremities, l_i, once the stars centres $P_{n,1}$ and $P_{m,2}$ have been made to coincide.

The application of the Voronoï PTV is here exemplified for $T = 1$. In Figure 9 it is possible to see the Voronoï diagrams of two consecutive images and the associated displacement field. It is worth to mention the way the Voronoï tessellations adapts itself to the presence of the discontinuity in the flow images caused by the free surface, allowing the detection of such flow boundary.

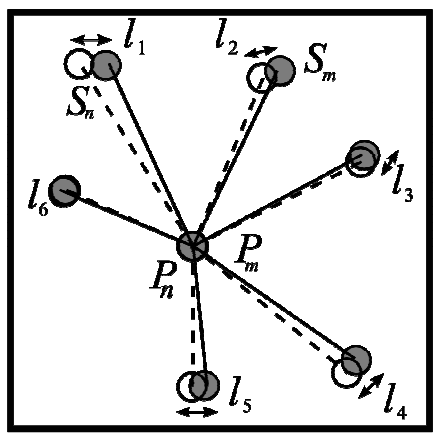

Figure 8: Determination of the median displacement of a Voronoï star

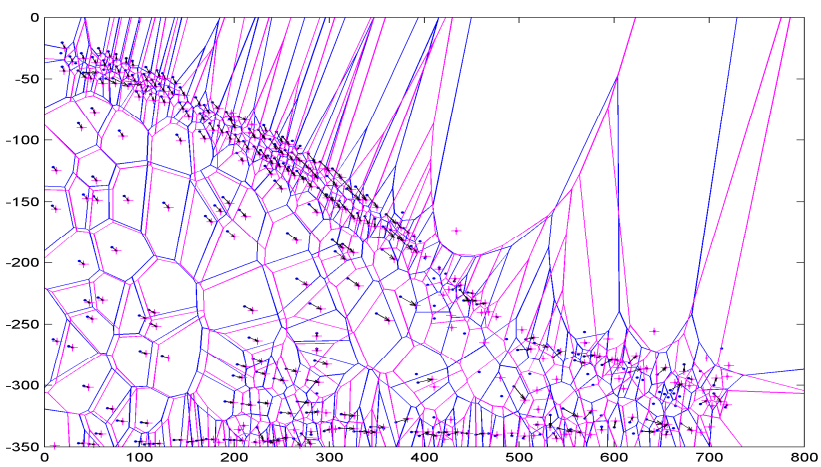

Figure 9: Voronoï diagram and displacement field associated. Blue line Voronoï diagram for $T = 0.945$ and pink line represents the Voronoï diagram for $T = 1$. Axis co-ordinates in pixels.

3.3 PTV Post-Processing

After detecting and tracking the particles a velocity field is obtained where each successfully detected particle will hold a velocity vector. As said before, due to the random dispersion of seeding particles in the flow the velocity field will be on a non-structured grid. In order to compare the velocity fields between different experiences it is therefore needed to refer the obtained velocity field to a structured grid. In this paper two methods are used: the binning process and the interpolation towards a predefined structured grid.

3.4 Binning Method

Let V_{ij} denote a non-structured velocity field between $a < x_i < b$ and $c < y_j < d$, as depicted on Figure 10a. Considering now the regular division of the intervals [a, b] and [*c*, *d*] in *n* equally spaced intervals as depicted in Figure 10b and here designated by bins. The binning method consists in replacing all the vectors inside a bin, by a characteristic vector (Figure 10c) [9].

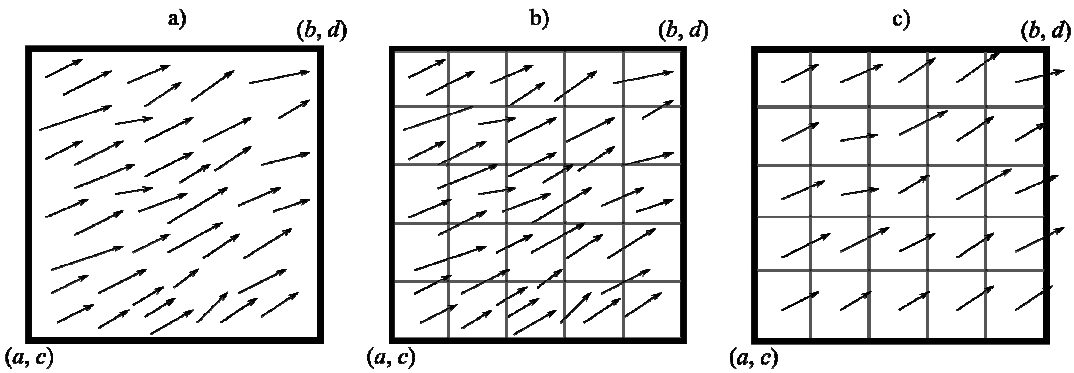

Figure 10: Velocity field and bin division of the flow image.

It is possible to see that each bin, *k*, will contain a finite number of velocity vectors. The binning method consists in replacing all the vectors inside a bin by their average:

$$v_k = \frac{1}{n}\sum_{i,j} v_{ij} \tag{9}$$

With this method it is possible to easily obtain a method to filter out outliers in each bin. This method consists in a three step operation. The first step is the computation of the bin average. The second is the identification of the outlier in the bin, and the third one is the computation of the new average without the outlier value. These set of operations is illustrated in Figure 11a to d.

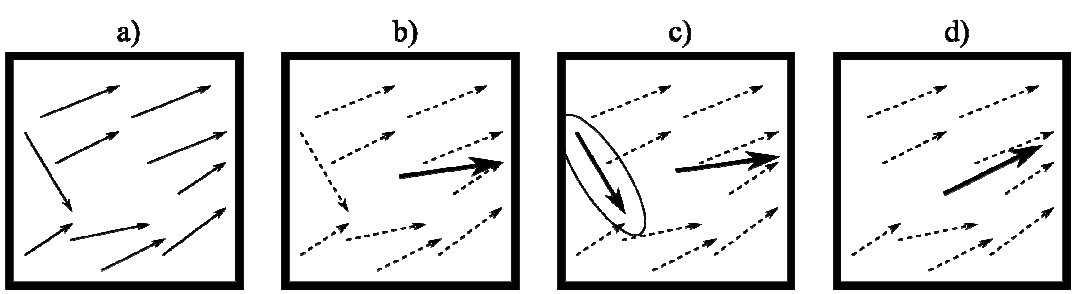

Figure 11: a) Bin with velocity vectors; b) Initial average calculation; c) Identification of outlier and d) Final average calculation without outlier vector.

The binning is in fact a spatial average that can lead to an artificial smoothing of the velocity field and so care must be taken when choosing the binning dimensions. A too large bin may mask important features of the flow. A too small bin may not contain data at all. For the dimensions of the bin two criteria are used: one is based on the evaluation of the obtained results in function of the number of bins without data and the other is based on the displacement of the tracked particles, in the time interval between images Δt. If u is a characteristic velocity of the flow, the bin size is estimated as:

$$\Delta x \sim \mathbf{int}(n \cdot u \cdot \Delta t) \tag{10}$$

Where n is a constant and **int** denotes the immediately largest integer.

3.5 Interpolation to a Regular Grid

Another way of structuring the grid is defining a structured grid of regular spacing as defined by equation (10) and interpolating to those grid points the non structured velocity field by means of a convenient interpolation method, as represented in Figure 12.

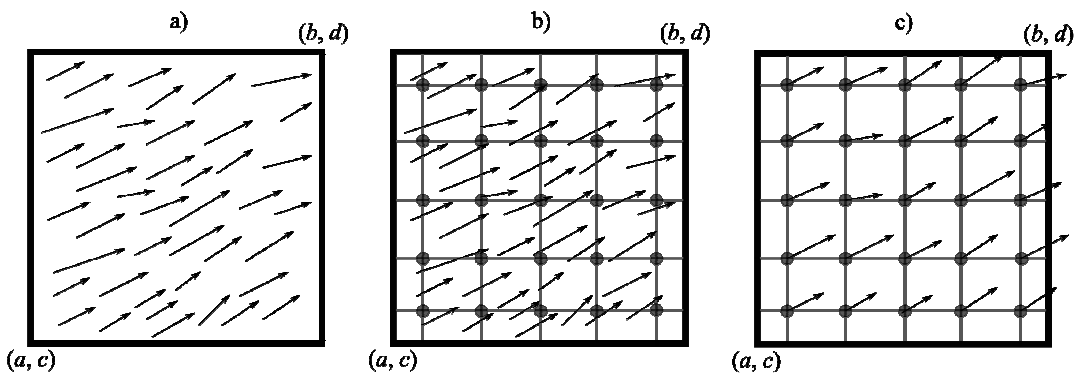

Figure 12: Velocity field and bin division of the flow image.

A triangular based liner interpolation method was chosen to obtain the velocity field values in the structured data grid [10].

Both data structuring techniques will be applied in the next examples, and compared.

4 EXPERIMENTAL SETUP

4.1 Dam Break Channel

The dam break channel of the Hydraulics Laboratory (Civil and Engineering Department, Université catholique de Louvain, Belgium) has 6 m long, 0.25 m width and its height is 0.50 m [11]. At the middle of a channel a gate divides the channel in two equal parts. The upstream part is filled with water and used as a reservoir; the downstream reach is used as test section. The gate moves downward pulled by a pneumatic jack. The opening time was measured to be 130 ms.The channel bottom is a flat and smooth wooden plate for the reservoir reach and a smooth flat glass to allow optical access for the test section. A channel photography and sketch are represented in Figure 13. To light the flow three 1000 W projectors placed over the channel (Figure 13).

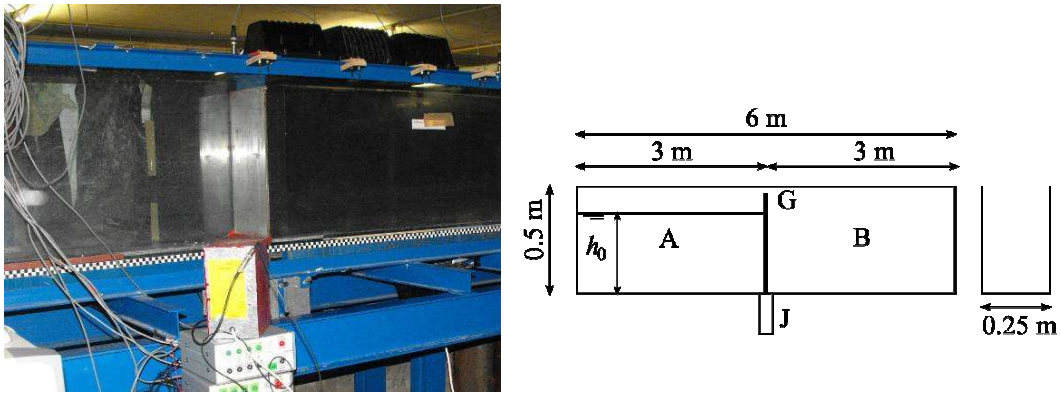

Figure 13: Dam break channel photography and sketch with dimensions (not at scale).

The upstream reservoir was filled with water up to an initial height of 0.325 cm. This reservoir was seeded with particles made of high density polyethylene (ρ/ρ_w = 0.94), with a diameter of 2 mm. Particles light reflection was improved by means of a white coating film. The combination between the light particle density and the denser white coating made the resulting particles roughly neutrally buoyant.

4.2 Imaging System

The images were acquired with a camera DALSA® DS21-1M150 having 1 Mpix resolution. This model is controlled by software and allows image acquisition just up to 150 frames per second at full resolution. In this study the acquisition frequency was set to 100 frames per second. Hardware limitations made the acquisition duration limited to 15 seconds, enough however for the study of the main features of a dam break flow. Lenses of 25 mm and 35 mm were used. The images were recorded on a PC for post processing and analysis.

5 OBTAINED RESULTS AND DISCUSSION

In order to apply the Voronoï Particle Tracking Velocimetry to the dam break flow two different time instants were chosen to describe the flow in the Near Field and the Far Field regimes. The chosen non-dimensional time instants for processing were $T = 1$ and $T = 7$. In order to obtain better statistics a time interval centred in the chosen non-dimensional time instants was used. This non-dimensional time interval was defined for the near field to be $\Delta T = \pm 0.11$ corresponding to a sampling of five images, and $\Delta T = \pm 0.275$ corresponding to 11 images sampling for the far field case.

5.1 Velocity Results T =1

For the near field case a sensibility analysis for the bin size was performed. The bins sizes were defined by equation (10) where n = 1, 2 and 3. In Table 1 the different parameters are expressed for a characteristic velocity of u = 13.68 pixels per time unit.

n	Δx (pix)	*# bins*
1	14	57 x 57
2	28	28 x 28
3	41	19 x 19

Table 1: Obtained bin size parameters for T = 1.

In Figure 14 a raw image of the flow for $T = 1$ and the corresponding non-structured velocity field is presented.

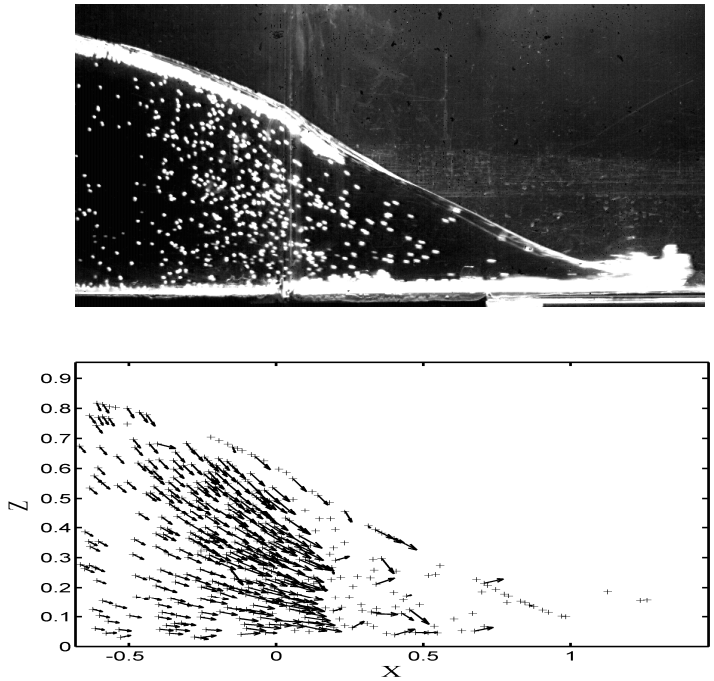

Figure 14: Flow image for $T = 1$ and corresponding velocity field obtained with PTV (non-structured grid)

The two structuring methods proposed, binning and interpolation, are here applied and the results compared. The obtained results are represented in Figures 14 to 16. When analyzing the bin size effect (Figure 15a, 16a and 17a) it is possible to see that with increasing bin size, (less bins) the flow field tend to be smoother, but with lesser spatial resolution.

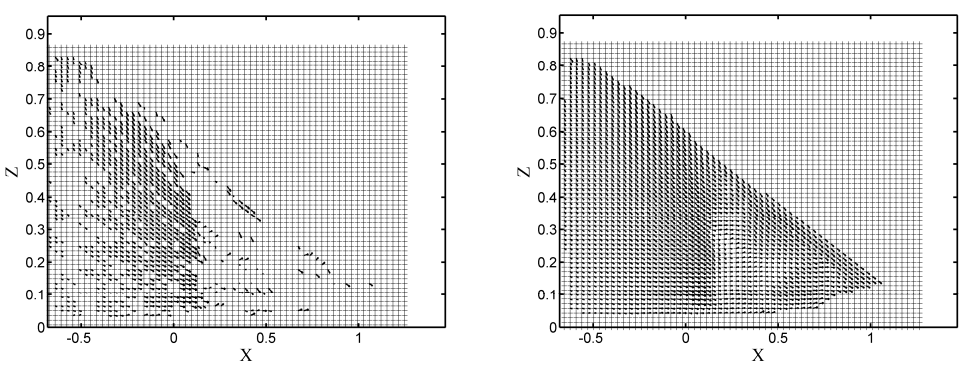

Figure 15: Velocity field for a structured grid of 61×61 points at $T = 1$ obtained by a) Binning Method; b) Interpolation.

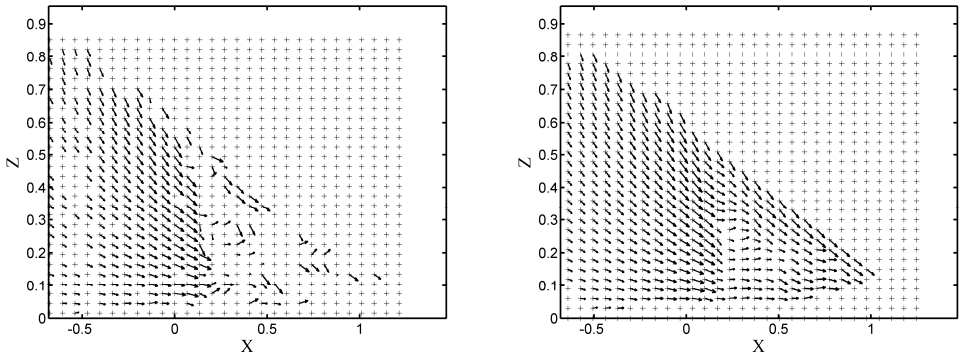

Figure 16: a) Velocity field for a structured grid of 29×29 points at $T = 1$ obtained by a) Binning Method; b) Interpolation.

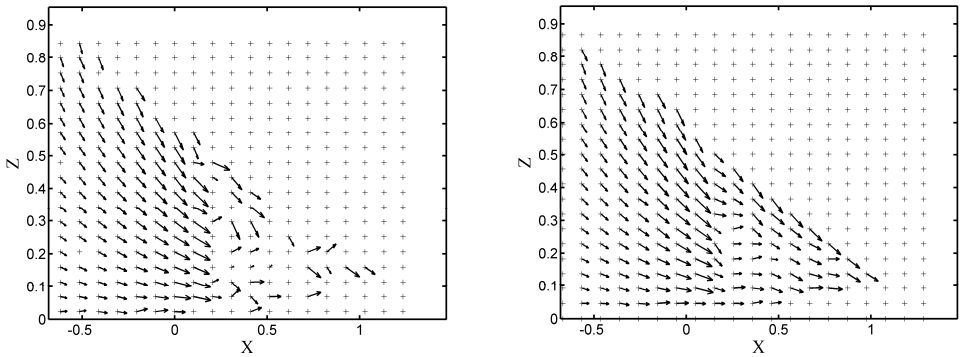

Figure 17: Velocity field for a structured grid of 19×19 points at $T = 1$ obtained by a) Binning Method; b) Interpolation.

With the binning method there are data only where particles are successfully detected and tracked. When considering the interpolation method one sees that this method determines values for the velocity field in regions of the flow where no particles where tracked. These features are put in evidence in Figure 18 showing velocity profiles at $X = 0$, i.e. at the gate section.

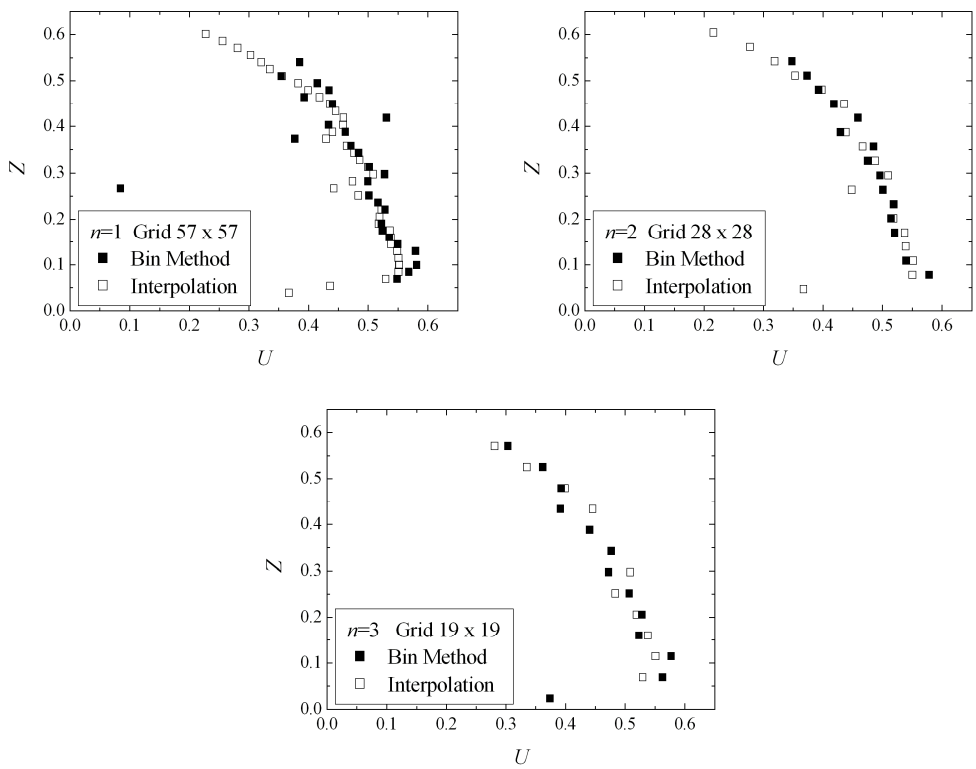

Figure 18: Comparison between binning and interpolation methods for different grid sizes.

From Figure 18 it results that for $n = 2$ one obtains a good compromise between spatial resolution and profile smoothing. This value was used in the next cases. It is also possible to see that the values obtained from the interpolation and the binning schemes used do agree well.

5.2 Velocity Results $T = 7$

The same analysis was performed for a different time instant of the dam break flow now corresponding to the far field conditions. The flow image corresponding to $T = 7$ is depicted in Figure 19 along with the corresponding velocity field obtained by PTV. The differences with the near field case ($T = 1$) are clearly seen. The flow now occupies the whole width of the image, the free surface slope is milder and the velocity field is practically parallel to the bed. The measured velocity are also different from the ones obtained for $T = 1$, namely the velocity scale to be used in equation (10) is now $u = 20.26$ pixels per unit time.

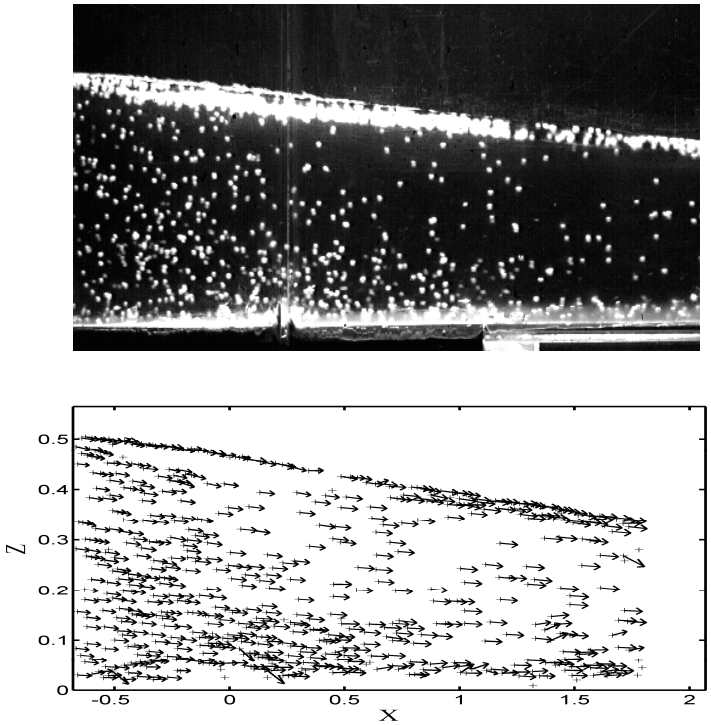

Figure 19: Flow image for $T = 7$ and corresponding velocity field obtained with PTV (non-structured grid)

Using $n = 2$ a structured grid of 24×24 points is obtained. The resulting velocity field was determined using both the binning and interpolation methods (Figure 20).

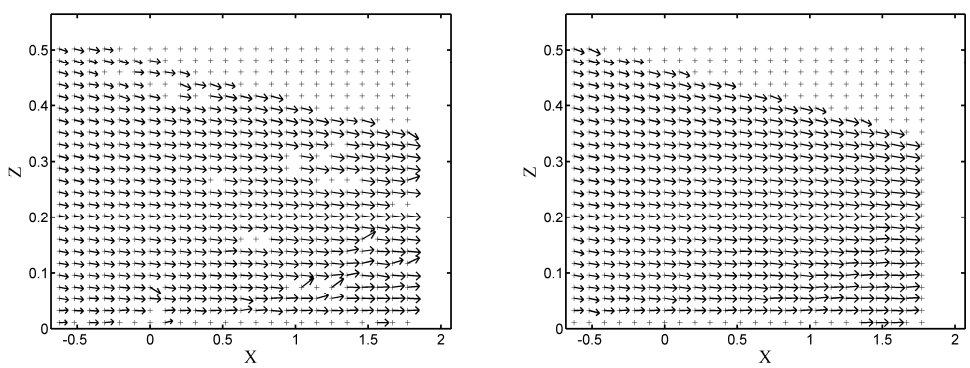

Figure 20: Velocity field for a structured grid of 24×24 points at $T = 7$ obtained by a) Binning Method; b) Interpolation

From Figure 20 it is possible to observe that the method based on the interpolation gives more uniform results than the binning method. On other hand, when using the interpolation method the whole flow region is filled whereas when using the binning method there are some points without data. Similarly the velocity profile at the gate section ($X = 0$) is plotted for the two methods. The results of the horizontal, U, and vertical components, W, are plotted in Figure 21. It is possible to conclude that the velocity field is practically parallel at this section and that $|U|>>|W|$.

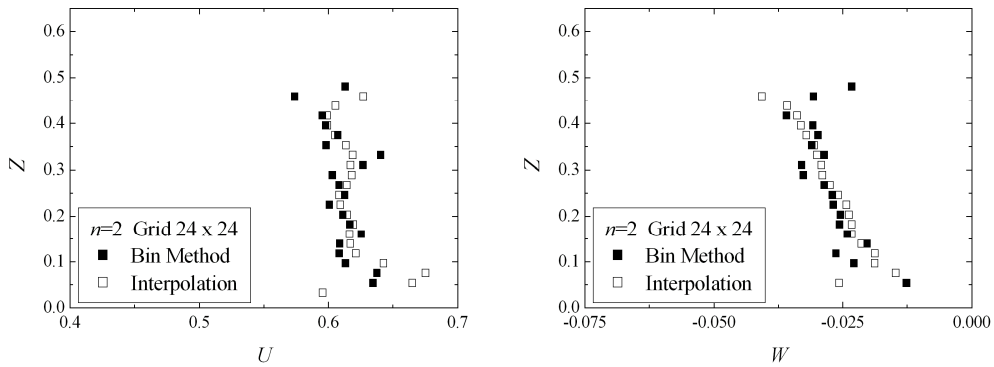

Figure 21: Velocity profiles at $X = 0$ and $T = 7$ for the two methods, binning and interpolation.

6 PARTICLE IMAGE VELOCIMETRY ANALYSIS

To complement this study the flow images referring to the far field case where also processed by a commercial Particle Image Velocimetry software package made by LaVision®. Particle Image Velocimetry (hereafter referred as PIV) is another approach to obtain the velocity field information by processing images of a flow seeded with particles. It is nowadays an established technique [12] with the main advantage of allowing the measurement of the whole field. Instead of tracking individual particles, PIV relies on image cross correlation between two consecutive images, hereafter referred as pair of PIV images. Each image of a PIV pair is divided in smaller areas called interrogation windows. Cross correlation between each interrogation window will hold a displacement vector, $\Delta\mathbf{x}$, and being the time interval between an image pair, Δt, the velocity vector for each interrogation window is then calculated by:

$$\mathbf{v} = \frac{\Delta\mathbf{x}}{\Delta t} \tag{10}$$

The dam break flow at $T = 7$ was analyzed with the PIV software. An iterative processing algorithm was used for the interrogation windows dimensions, and the processing parameters are resumed in Table 2.

Initial interrogation window size	64×64 pixels^2
Final interrogation window size	32×32 pixels^2
Interrogation window overlap	50%
Number of iterations	2

Table 2: Parameters used for the PIV data processing.

The use of interrogation windows will result in a structured grid for the flow field and the PIV results for $T = 7$ will be compared with the ones illustrated in Figures 19-21 that were obtained with the Particle Tracking Velocimetry for the same time instant. Figure 22 shows the flow field obtained through PIV analysis with interrogation windows of size described in Table 2.

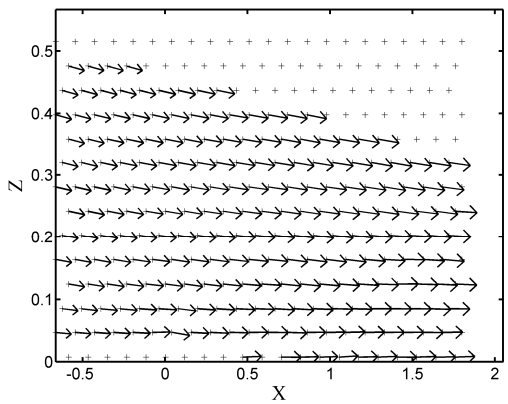

Figure 22: Velocity field obtained with PIV at T = 7. Only one out of three vectors plotted

To better compare the results from the different techniques (PTV and PIV) the velocity profiles obtained at X = -0.5, X = 0 and X = 0.5 are shown in Figures 23 to 25. It is possible to see that the obtained results agree well.

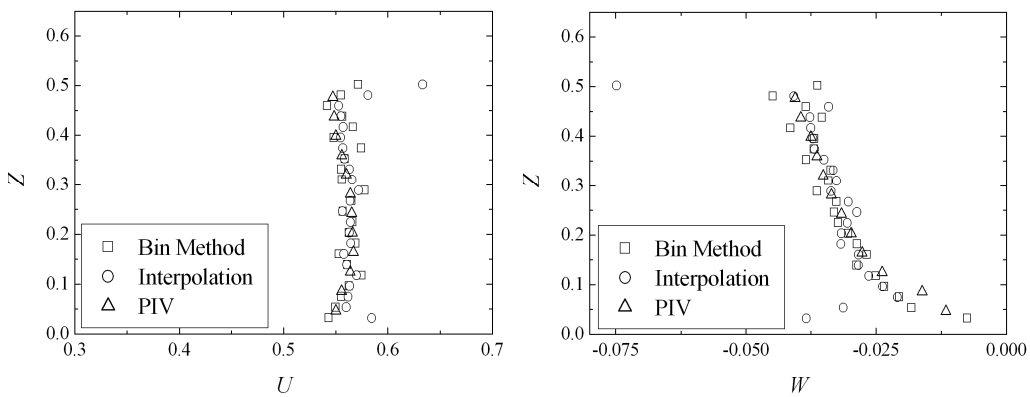

Figure 23: Velocity profiles at X = -0.5.

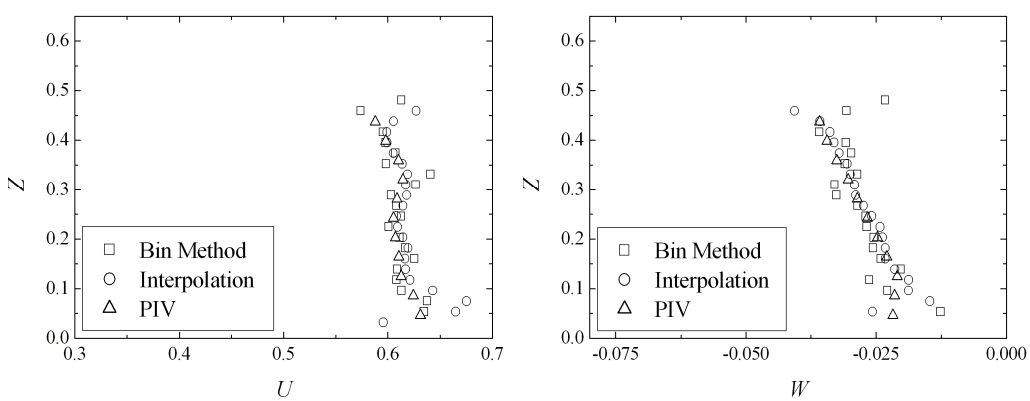

Figure 24: Velocity profiles at X = 0.0.

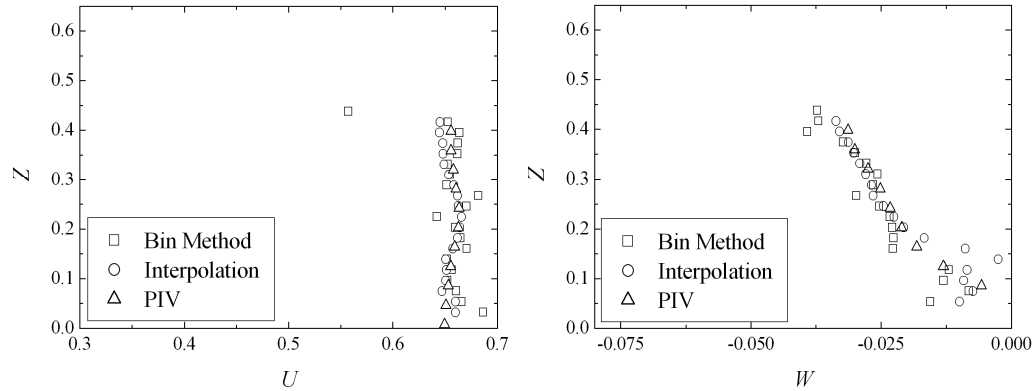

Figure 25: Velocity profile at X = 0.5.

7 CONCLUSIONS

The analysis of the dam break flow, an example of severe transient flow, was made in the scope of this paper by means of imaging analysis. The information about the velocity field was extracted using a Particle Tracking Velocimetry Algorithm. In order to compare the obtained velocity values between experiences it is useful to have the PTV velocity field referred to a regular grid. Since the velocity field obtained with PTV is on a non-structured grid two different strategies were used to obtain the velocity field in a structure grid. One based on the binning method and the other based on linear interpolation. Both methods gave similar results but care must be taken when using the interpolation method, since it is possible to obtain velocity field values in regions where no physical velocities were measured.

For obtaining a structured grid a criterion based on multiples of particle displacement was used. A larger grid will result on a smoother velocity field but with lesser spatial resolution, on the other hand, the use of a smaller grid can result in a “noisy” velocity field. For the tested cases a grid that was twice the maximum particle’s displacement was used as a compromise between spatial resolution and profile averaging.

The flow images where also analyzed with a PIV algorithm and the obtained results were compared with the ones obtained with the structured PTV. It was possible to see that the two methods gave very similar results but PIV offered a higher spatial resolution than the structured PTV due to the interrogation window overlap. This fact suggests that the criterion for defining the grid size can be redefined and instead of using the maximum particle displacement an average displacement can possibly be an adequate solution.

8 ACKNOWLEDGMENTS

The present work was made possible by a PhD support for the first author under scholarship SFRH/BD/36023/2007 from the Fundação para a Ciência e Tecnologia, Portugal.

The PIV software used was funded by the Convention 2.4.526.08 du Fonds de la Recherche Fondamentale Collective (Fonds de la Recherche Scientifique), Belgium.

REFERENCES

[1] R.D. Keane and R.J. Adrian, Theory of Cross-correlation analysis of PIV images. Applied Scientific Research **49**, pp. 191-215 (1992)

[2] C. Tropea, A. L. Yarin and J. F. Foss (Eds). Handbook of Experimental Fluid Mechanics, Springer, (2007)

[3] R. Aleixo, S. Soares-Frazão and Y. Zech, Velocity-field measurements in a dam-break flow using a PTV Voronoï imaging technique (submitted to Experiments in Fluids)

[4] H. Capart, D.L. Young and Y. Zech, Voronoï imaging methods for the measurement of granular flows. Experiments in Fluids, **32**, pp. 121-135 (2002)

[5] J.J. Stoker, Water waves: the mathematical theory with applications, Interscience, (1957)

[6] S. Soares-Frazão, S., Y. Zech, Dam-break flow through an idealised city. Journal of Hydraulic Research, **46**(5), pp. 648-658 (2008)

[7] G. Lauber, W.H. Hager, Experiments to dambreak wave: horizontal channel. Journal of Hydraulic Research, 36, 291-307, (1998)

[8] Y.A. Hassan, R.E Canaan, Full field bubbly flow velocity measurements using a multiframe particle tracking technique. Experiments in Fluids 12, pp. 49-60, (1991)

[9] R. Aleixo, B. Spinewine, S. Soares-Frazão and Y. Zech, Non-intrusive measurements of water surface and veloc-ity profiles in a dam-break flow. Proceedings of the 33rd Inter. Assoc. of Hydraulic Eng. & Research (IAHR) Biennial Congress Vancouver, Canada, August 9-14 (2009)

[10] D.F. Watson and G.M. Philip, Triangle Based Interpolation, Mathematical Geology, **16**(8) pp. 779-795 (1984)

[11] B. Spinewine, Y. Zech, Small-scale laboratory dam-break waves on movable beds, Journal of Hydraulic Research Vol. **45** Extra Issue, pp. 73-86 (2007)

[12] M. Raffel, C. Willert, S. Werely and J. Kompenhans, Particle Image Velocimetry – A practical guide 2nd Edition. Springer (2007)